Langmuir

Article

pubs.acs.org/Langmuir

Environment-Dependent Guest Exchange in Supramolecular Hosts

Longyu Li and S. Thayumanavan*

Department of Chemistry, University of Massachusetts, 710 North Pleasant Street, Amherst, Massachusetts 01003-9336, United States

Supporting Information

ABSTRACT: Dynamic exchange of guest molecules, encapsulated in host assemblies, is a phenomenon in supramolecular chemistry that has important implications in several applications. While the mechanism of exchange in micellar assemblies has been previously investigated, the effect of host and guest environment upon the guest-exchange dynamics has received little attention, if any. In this paper, we study the guest-exchange mechanism in pH-sensitive nanogels along with pH-insensitive nanogels as a control. By systematically comparing the behavior of these nanogels, we show that size, concentration, and hydrophobicity can all play a critical role in guest-exchange dynamics. More importantly, these studies reveal that the dominant mechanism of guest exchange can intimately depend on environmental factors.

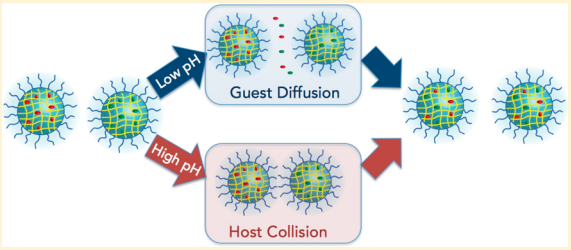

INTRODUCTION

Nanocontainers that can bind and hold hydrophobic molecules have attracted significant interest due to implications in areas such as self-healing materials and drug delivery.[1−3] Among the factors that are taken into account while arriving at a molecular design for these containers, encapsulation stability is often considered a critical one.[4,5] Encapsulation itself is often defined by the loading capacity of the host, i.e., the amount of guest molecule that a host assembly can hold. This capacity is dictated by the thermodynamic distribution coefficient of the guest molecule between the host and the solvent.[6−8] A feature that has not received much attention involves the guest-exchange dynamics. This is important, as this is a direct and arguably the most rigorous indicator of encapsulation stability of a host assembly.[9] Considering the diversity of the environments that a supramolecular assembly encounters in a typical biological system, it is important that we understand the influence of these external environmental factors upon encapsulation stability. In this paper, we show that the mechanism of guest-exchange dynamics and thus the factors that affect encapsulation stability can greatly vary with environmental changes.

Three limiting scenarios exist for the mechanism of guest exchange: (i) collision−exchange−separation mechanism, (ii) exit−re-entry mechanism, and (iii) fission−recombination mechanism.[10−16] The first mechanism is collision-based, where the guest exchange occurs only because of a collision between two host assemblies. The rate of this process mostly depends on the effective collision frequency. The second pathway is diffusion-based, where the guest-exchange rate depends on the ability of guest to exit and enter from the host assemblies. The third mechanism involves fragmentation of the host assembly into two smaller entities as the first step, followed by a recombination to regain the original host assembly (Figure S1, Supporting Information). To simplify the possibilities, we chose to use host assemblies that are based on cross-linked polymer nanogels, which do not lend themselves to the third possibility. The cross-linking feature of nanogels obviates the fission possibility, and thus, the third mechanism can be ruled out in this case. The two viable pathways for the host assembly are illustrated in Figure 1. Between these

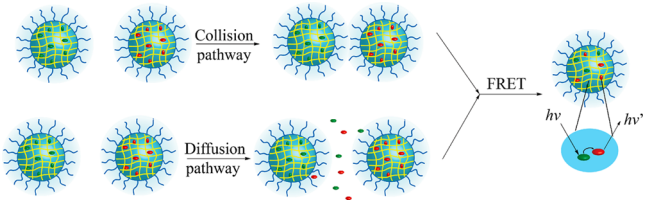

Figure 1. Schematic representation of two possible mechanisms for guest exchange between cross-linked nanogels: (a) the collision−exchange−separation mechanism, also called the collision-based mechanism, and (b) the exit−re-entry mechanism, also called the diffusion-based mechanism.

pathways, although the kinetic orders of these mechanisms are different, it is difficult to quantify the order of a molecular exchange process, as this is not a chemical reaction. Here, we design a series of experiments to probe the possible pathways for guest exchange in these polymeric nanogels.

We use the recently reported fluorescence resonance energy transfer (FRET) as the tool to interrogate the guest-exchange process,[17] which has proved to be quite a robust method for a variety of host−guest assemblies.[18−25] Briefly, a hydrophobic

Received: July 13, 2014
Revised: September 10, 2014
Published: September 22, 2014

FRET pair, 3,3′-dioctadecyloxacarbocyamine perchlorate (donor) and 1,1′-dioctadecyl-3,3,3′,3′-tetramethylindocarbocyanine perchlorate (acceptor), were independently encapsulated in otherwise similar nanogel hosts. When these solutions were mixed, the emission spectrum of the mixed solution in response to donor excitation at 450 nm was monitored over time. No FRET would be observed if the two dye molecules are stably encapsulated and continue to be in their separate nanocontainers, since the distance between the two dye molecules is much higher than their Förster radii. On the other hand, if the guest exchange between the host and its surroundings was significant, the extent of FRET would evolve, as the guest composition in the nanogel changes over time.

EXPERIMENTAL SECTION

General Methods. 2,2′-Dithiodipyridine, 2-mercaptoethanol, poly(ethylene glycol) monomethyl ether methacrylate (PEGMA, M_w 450), 2-(diisopropylamino)ethyl methacrylate (DPA), D,L-dithiothreitol (DTT), 1,1′-dioctadecyl-3,3,3′,3′-tetramethylindocarbocyanine perchlorate (DiI), 3,3′-dioctadecyloxacarbocyanine perchlorate (DiO), 4-cyano-4-(phenylcarbonothioylthio)pentanoic acid, and other conventional reagents were obtained from commercial sources and were used as received without further purification. 2,2′-Azobis(isobutyronitrile) (AIBN) was purified by recrystallization from ethanol. Pyridyl disulfide ethyl methacrylate (PDSEMA) was prepared using a previously reported procedure.[26] Phosphate buffer solutions were prepared by using monosodium phosphate and disodium phosphate. The buffer strength was constant at 10 mM. The pH value was determined via the Accumet AB 15/15+ benchtop pH meter. ^{1}H NMR spectra were recorded on a 400 MHz Bruker NMR spectrometer using the residual proton resonance of the solvent as the internal standard. Chemical shifts are reported in parts per million (ppm). Molecular weights of the polymers were estimated by gel permeation chromatography (GPC) using PMMA standard with a refractive index detector. Dynamic light scattering (DLS) measurements were performed using a Malvern Nanozetasizer. UV−visible absorption spectra were recorded on a Varian (model EL 01125047) spectrophotometer. The fluorescence spectra were obtained from a JASCO FP-6500 spectrofluorimeter. Transmission electron microscopy (TEM) images were taken using a JEOL 2000FX at 200 kV. All experiments were carried out at ambient temperature, unless otherwise mentioned.

Synthesis of Random Copolymer. Random copolymer **P2**, containing DPA groups, was synthesized according to a previously reported procedure.[27] A mixture of 4-cyano-4-(phenylcarbonothioylthio)pentanoic acid (12.0 mg, 0.043 mmol), PDSMA (150.0 mg, 0.588 mmol), PEGMA (215.0 mg, 0.453 mmol), DPAMA (130.0 mg, 0.609 mmol), and AIBN (1.5 mg, 0.010 mmol) was dissolved in THF (1.0 mL) and degassed by performing three freeze−pump−thaw cycles. The reaction mixture was sealed and then transferred into a preheated oil bath at 65 °C and stirred for 10 h. To remove unreacted monomers, the resultant mixture was precipitated in cold diethyl ether (20 mL) and redispersed in THF three times to yield the random copolymer **P2** as a waxy solid. GPC (THF) M_n: 10.6 kDa. $Đ$: 1.44. ^{1}H NMR (400 MHz, $CDCl_3$) δ: 8.46, 7.67, 7.10, 4.35−4.09, 3.94−3.37, 3.02, 2.62, 2.04−1.64, 1.43−0.87. The molar ratio (PDS/PEG/DPA) was determined to be 34%/28%/38% by integrating the methoxy protons in the polyethylene glycol unit (δH_d = 3.37 ppm), the aromatic protons in the pyridine (δH_a = 8.46, δH_b = 7.67, δH_c = 7.10), and the methylene protons next to the nitrogen in DPA units (δH_e = 2.62, δH_f = 3.02).

Preparation of Nanogels Contaning DiI/DiO. Polymer (10 mg) was dissolved in 1 mL of water, and the pH was adjusted to around 10 through the addition of NaOH aqueous solution (1 M). Then 0.04 mL of DiI in acetone stock solution (5 mg/mL) or 0.08 mL of DiO in acetone stock solution (2.5 mg/mL) was added into the polymer solution (0.2 mg of each dye for 10 mg of polymer in 1 mL of water). The final dye concentration was about 0.2 mmol/L. The mixed solution was stirred overnight at room temperature, open to the atmosphere to allow the organic solvent to evaporate. Then a measured amount of DTT (0.2 μmol for 15 mol % against PDS groups) was added. After stirring for 4 h, insoluble DiI/DiO was removed by filtration and the pyridothione byproduct was removed from the nanogel solution by extensive dialysis using a membrane with a molecular weight cutoff of 7000 g/mol. Finally, nanogel stock solutions with a concentration of 1 mg/mL were prepared for further studies.

Mixing of Nanogel-Encapsulated Dyes. Nanogel containing DiI and nanogel containing DiO were mixed in phosphate buffer solution at ambient temperature and at a certain pH value such that the total volume was 1 mL. The pH did not change after mixing. The fluorescence spectra were recorded using a 450 nm excitation wavelength. At the same time, absorption spectra were also measured for all samples to ensure that there is no loss of dye molecules due to precipitation. The FRET ratio $I_a/(I_a + I_d)$, where I_a and I_d are the fluorescence intensities of the acceptor (DiI) and the donor (DiO), respectively, was plotted against time to show the dynamics of the dye exchange in nanogel solution. The leakage coefficients (Λ) were calculated on the basis of the slopes from four earlier points in the linear regime. In the case of very fast guest exchange, the time frame for obtaining these four data points is shorter.

RESULTS AND DISCUSSION

Two cross-linked polymeric nanogels were used in this study. The first nanogel (**NG-C**) is based on a random copolymer (**P1**), formed from a hydrophilic oligoethylene glycol (OEG) functionalized methacrylate monomer and a hydrophobic pyridyl disulfide (PDS) functionalized methacrylate monomer (Scheme 1). The second nanogel (**NG**) and its precursor (**P2**)

Scheme 1. Structure of Polymers P1 and P2, Nanogels NG-C and NG, and the Dye Molecules DiO and DiI

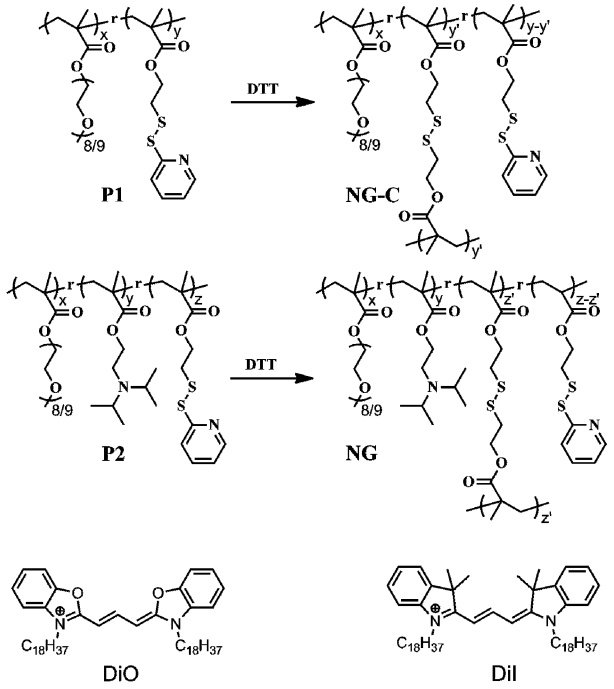

contain a diisopropylamine (DPA) functionalized methacrylate as a comonomer in addition to the OEG- and the PDS-functionalized monomers.[27] The size of these two types of nanogels at neutral pH was found to be very similar (Figure 2).

First, we were interested in understanding the mechanism of guest exchange in the control nanogel **NG-C**, which is not

dx.doi.org/10.1021/la502760c | Langmuir 2014, 30, 12384−12390

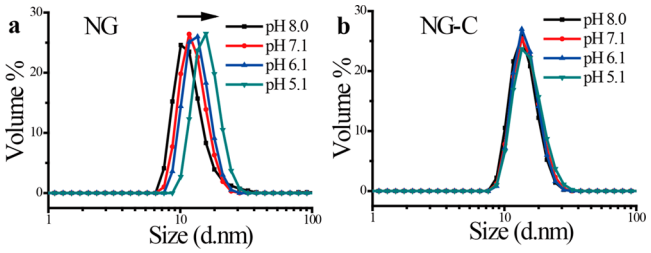

Figure 2. Size distribution of nanogel at different pH values via DLS measurements: (a) **NG** with 30% cross-linking density and (b) **NG-C** with 20% cross-linking density.

sensitive to the external environment, as this provides the baseline for our study. Among the collision- and diffusion-based pathways, the former pathway should clearly depend on the concentration of the nanogel. One would expect strong and positive correlations between the collision frequency and the concentration of nanogels in solution. We used the FRET-based method, which provided a measure of the dye exchange rate in the form of the leakage coefficient (Λ), which can be obtained as the initial slope of the linear fit (earlier four points in the linear regime) by plotting the FRET ratio $I_a/(I_a + I_d)$ against time, where I_a and I_d are the fluorescence intensities of the acceptor (DiI) and the donor (DiO) respectively. The concentrations of the nanogels were varied as 0.05, 0.10, and 0.15 mg/mL for both **NG-C** containing DiI and **NG-C** containing DiO at pH 7.1. Figure 3c shows that there was indeed a faster evolution of FRET with time in the nanogels with a concentration of 0.15 mg/mL, compared to those with a concentration of 0.05 mg/mL (Figure 3a) and 0.10 mg/mL (Figure 3b). Λ values of 0.0192, 0.0284, and 0.0315 min^{-1} were observed for the concentrations of 0.05, 0.1, and 0.15 mg/mL, respectively, indicating that the guest exchange between nanogels indeed increased with increasing concentration (Figure 3d). These data provide the initial evidence that the guest exchange in these control nanogels happens via the collision-based mechanism as the dominant pathway.

Additionally, the size of the nanogel would also impact guest exchange, if the collision-based mechanism was the dominant mechanism for guest exchange, since the collision frequency would be affected by the size of nanogels. The pH-sensitive nature of the DPA moieties endows **NG** with pH-dependent size variations in this nanogel. The size of **NG** increases with decreasing pH, while the size of **NG-C** does not change with pH (Figure 2). Figure 2a shows that the sizes of **NG** increased from 10 to 18 nm when the pH changed from 8.0 to 5.1. The observed size increase in **NG** is attributed to the protonation of the DPA units, which presumably results in the swelling of the nanogels due to electrostatic repulsion between these positively charged DPA groups inside. As the size of **NG** varies with pH, we expected that the dye-exchange rate would also change with the pH.

Figure 4a shows that there is a rapid evolution of FRET with time for **NG** at pH 8.0. On the other hand, **NG** at pH 6.4 exhibits little change in FRET ratio with time and thus shows very slow dye exchange (Figure 4b). Thus, the exchange rate indeed decreased from a Λ value of 0.080 min^{-1} at pH 8.0 to 0.004 min^{-1} at pH 6.4 (Figure 4d). These results are consistent with the collision-based mechanism, as the size of **NG** indeed affected the rate of guest exchange, providing further evidence that the dominant guest exchange in nanogels might happen via the collision-based mechanism. It should be noted, however, that while the collision frequency is expected to decrease with increase in size, because of the slower diffusion (via the Stokes−Einstein equlation), it is also known that the collision frequency can increase with an increase in size.[28] One possible explanation is that the number of effective collisions, i.e., collisions that result in guest exchange, decrease with an increase in size. This is reasonable, as the effect of the reduced diffusion could potentially reduce the effective collisions. This explanation is consistent with the results but remains

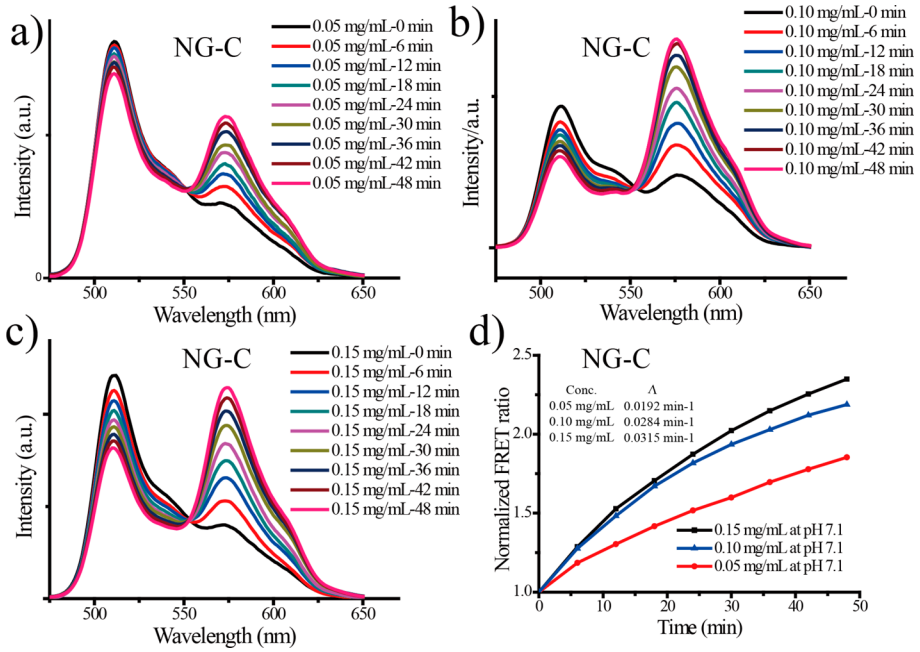

Figure 3. Fluorescence evolution when **NG-C** respectively containing DiI and DiO are mixed in solutions at pH 7.1: (a) 0.05 mg/mL, (b) 0.10 mg/mL, and (c) 0.15 mg/mL. (d) Comparison of the dynamics of guest exchange between **NG-C** with different concentrations at pH 7.1.

dx.doi.org/10.1021/la502760c | *Langmuir* 2014, 30, 12384−12390

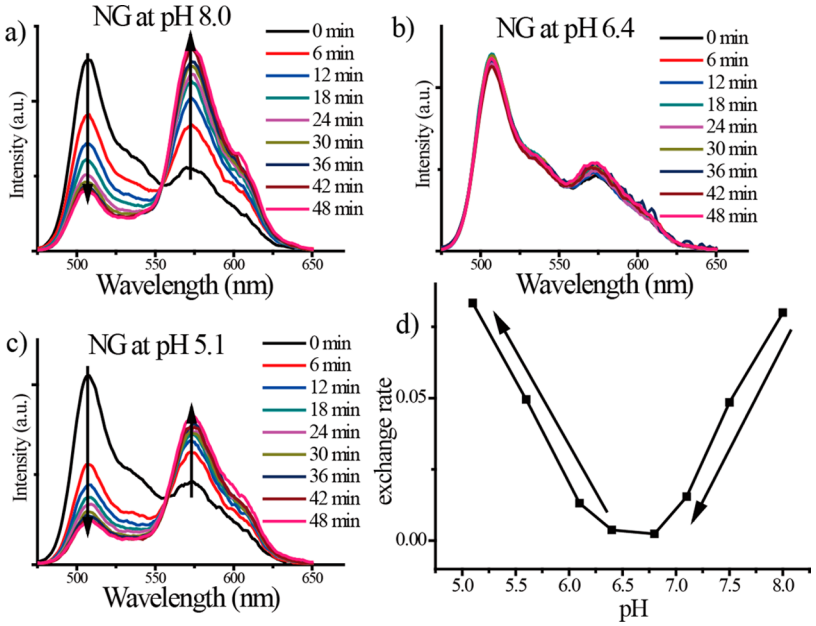

Figure 4. Fluorescence evolution when two **NG** solutions independently containing DiI and DiO dye molecule as guest are mixed in solutions at different pH values: (a) pH 8.0, (b) pH 6.4, and (c) pH 5.1. (d) Guest-exchange rates between **NG** at different pH values. The concentration of each nanogel was 0.10 mg/mL.

provisional, as there are no established quantitative relationships to this effect at this point.

Interestingly, however, an unexpected change in the FRET evolution occurs below pH 6.4, even though the size-increase is observed through the entire pH range from 8.0 to 5.1. From pH 6.4 to 5.1, the FRET evolution was found to increase (Figure 4c). Figure 4d shows that the exchange rate systematically increases with decreasing pH from 6.4 to 5.1. The Λ value of 0.004 min^{-1} at pH 6.4 increased back to 0.083 min^{-1} at pH 5.1. Since the size of the nanogel increases with decreasing pH, including at this pH range, these results are not consistent with the collision-based mechanism. Therefore, it is possible that the diffusion-based pathway is the dominant operating mechanism in this scenario, providing the first indication that there might be an environment-dependent change in mechanism. However, a few alternating possibilities need to be considered prior to reaching this conclusion.

First, it is possible that the dye molecules themselves have a certain pH-dependent solubility and thus is affecting the guest molecule exchange in the collision state. To test this possibility, we investigated the pH-dependence of guest-exchange dynamics in **NG-C**, where the size of the nanogel does not change with pH. Figure 5a,b shows that there was indeed similar evolution of FRET with time in the nanogels at pH 8.0 and 7.1, while a slightly faster FRET evolution was observed at pH 6.1 (Figure 5). We attribute the small pH-dependence to the possibility that the solubility of DiI and DiO molecules may vary at different pH values. The solubility may be improved a bit at low pH due to the presence of tertiary amine (Scheme 1), leading to easier dye exchange during the collision. Note that we do not observe any significant dye loss in the nanogel during our FRET experiments, which suggests that the repulsion between these positively charged dyes and protonated **NG** at lower pH might be very small. Two features are noteworthy in these results: first, the magnitude of difference in exchange dynamics is too small compared to those observed with **NG** and, therefore, does not account for the results observed with

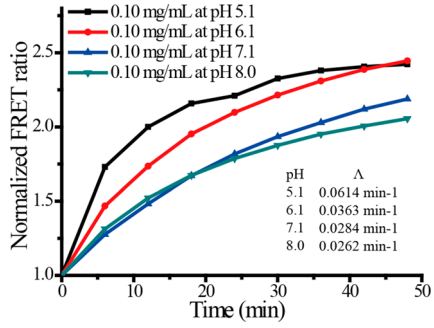

Figure 5. Comparison of the dynamics of guest exchange between **NG-C** with 0.10 mg/mL at different pH values.

NG. Second, the guest-exchange kinetics continues to increase with pH and there is no change in the trend after pH 6.4. These results suggest that the results observed in **NG** are not due to the inherent difference in dye molecule behavior at different pH values.

We hypothesized next that the observed change in pH-dependence trend at pH 6.4 could perhaps be explained by a change in the hydrophobicity of the nanogel interior, i.e., the host properties. It is reasonable to anticipate that the protonation of DPA groups would decrease the hydrophobicity of the nanogel.[29] Pyrene's fluorescence properties are greatly dependent on its microenvironment.[30,31] Specifically, the ratio of the intensities between the first and the third peaks (I_1/I_3) in the pyrene emission spectrum can be used to determine the polarity of the dye's microenvironment. The value of this ratio can range from 1.9 in polar solvents to 0.6 in certain hydrocarbon solvents. We utilized this dye as the guest molecule to probe the hydrophobicity of the microenvironment within the nanogel interiors. Aqueous buffer solutions of **NG** containing 2 wt % pyrene were prepared for this purpose at different pH values. A sample fluorescence spectrum of nanogel is shown in Figure 6a. The hydrophobicity of nanogel at different pH values was studied by calculating the intensity ratio

dx.doi.org/10.1021/la502760c | *Langmuir* 2014, 30, 12384−12390

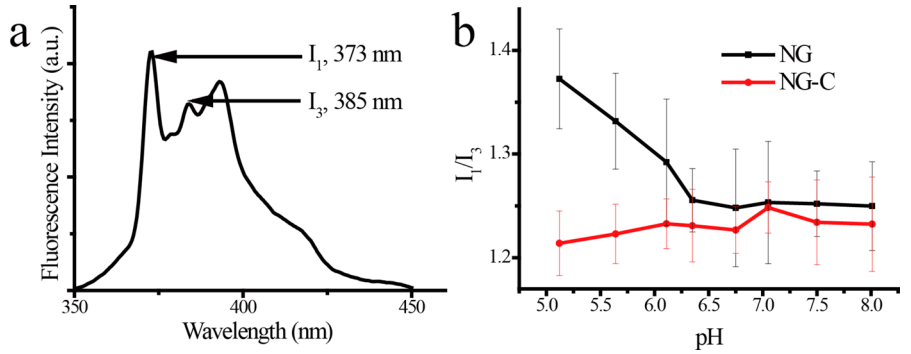

Figure 6. Effect of pH on the hydrophobicity. (a) Fluorescence emission spectrum measured for nanogel **NG-C** loading 2 wt % pyrene and (b) calculated I_1/I_3 ratios for nanogels at different pH values (black, **NG**; red, **NG-C**).

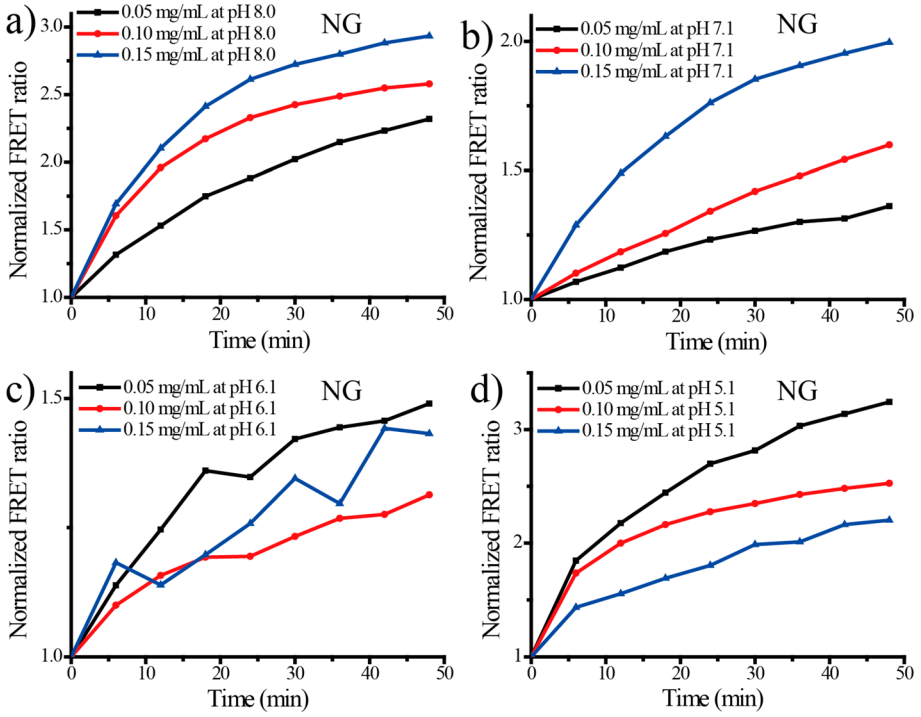

Figure 7. Comparison of the dynamics of guest exchange between **NG** of different concentrations (0.05, 0.10, and 0.15 mg/mL) at (a) pH 8.0, (b) pH 7.1, (c) pH 6.1, and (d) pH 5.1.

of the first and third emission peaks of pyrene, commonly referred to as the I_1/I_3 ratio. Figure 6b shows the variations in I_1/I_3 of pyrene encapsulated in **NG** at different pH values. When the pH was reduced from 8.0 to about 6.4, the I_1/I_3 remained constant around 1.25. This value suggests that the nanogel interior is quite hydrophobic. However, when the pH was further decreased, a steady increase in the I_1/I_3 value was observed, suggesting that the microenvironment of the dye is becoming increasingly polar. The I_1/I_3 ratio at pH 5.1 was found to be about 1.37. On the contrary, pyrene in the control nanogel **NG-C** (that lacks the DPA units) did not exhibit any discernible change in the I_1/I_3 ratio over the same pH range of 5.1−8.0, suggesting that the hydrophobicity of these nanogels was not pH-dependent.

While the environment inside **NG** was quite hydrophobic between pH 8.1 and 6.4, it became less hydrophobic when the pH value decreased from 6.4 to 5.1, which indicates that the ability of **NG** at these pH values to encapsulate the DiI or DiO molecules could be greatly depleted. Our studies with the control nanogel **NG-C** also suggest that the solubility of these dye molecules can be slightly improved at lower pH. Therefore, the dye might be able to exit one nanogel and diffuse through the solvent to re-enter another; i.e., the diffusion-based mechanism is possible in this case. Thus, these results suggest that the guest exchange is primarily based on the collision-based mechanism from pH 8.0 to 6.4, but changes to a diffusion-based mechanism below pH 6.4.

To further test this possibility, we investigated the effect of nanogel concentration on the guest-exchange rate at different pH values in **NG**. We varied the concentrations of **NG** samples (0.05, 0.1, and 0.15 mg/mL) and studied their FRET evolution at pH 5.1, 6.1, 7.1, and 8.0. Figure 7a,b shows that the exchange rates increase with nanogel concentration at both pH 7.1 and 8.0. This suggests that the guest exchange at these pH values indeed occurred mostly via the collision-based mechanism. However, while there is no clear trend at pH 6.1 (Figure 7c), the guest-exchange rate became slower with increasing concentration at pH 5.1, as Λ values of 0.098, 0.083, and

dx.doi.org/10.1021/la502760c | *Langmuir* 2014, 30, 12384−12390

0.046 min^{-1} were observed for nanogel concentrations of 0.05, 0.1, and 0.15 mg/mL, respectively (Figure 7d). Note that in a diffusion-based mechanism, the diffusion rate of dye out from the nanogel should depend on the concentration of nanogels in solution. At higher concentrations, the concentration of the host nanogel is higher, while the concentration of the dye is very low at all these concentrations. In this case, the driving force for the guest molecules to diffuse into the solvent from the host nanogel is lower at higher host concentrations. Therefore, the observed decrease in guest-exchange rate with the increasing nanogel concentration supports the assertion that a diffusion-based mechanism is dominant at pH 5.1.

If our hypotheses were correct, it should also follow that there should not be any change in the mechanism of guest exchange in **NG-C**, as the hydrophobicity of its interior does not change with pH. To perform this control experiment, we investigated the pH-dependent trends at different concentrations of **NG-C**. The concentration dependence of guest exchange was similar for this nanogel at all pH values (Figure S6–S8, Supporting Information). Indeed, the FRET evolution increased with concentration at all four pH values (Figure S9, Supporting Information), indicating that the guest-exchange rate indeed increased with the increasing concentration. This suggests that the operating mechanism is collision-based and is not dependent on pH in the pH-insensitive nanogel **NG-C**. The results from the control nanogel are consistent with our conclusions for the pH-sensitive nanogels **NG**.

CONCLUSIONS

In summary, we have designed a series of experiments to study the guest-exchange mechanism in pH-sensitive nanogels along with pH-insensitive nanogels as a control. We have shown that the dominant mechanism for guest exchange in these pH-insensitive nanogel hosts is collision-based. Perhaps, the most important take-home message of this work is that the mechanism of guest exchange in the pH-sensitive host–guest assemblies can change on the basis of the microenvironment of the host. When the nanogel interior is hydrophobic, the collision-based mechanism is the dominant pathway. However, when the interior is sufficiently hydrophilic, the dominant mechanism changes to a diffusion-based one. From an even broader perspective, it is important to recognize that both the intrinsic factors, such as size and interior environment of the host assemblies, and the extrinsic factors, such as pH and concentration, can have significant impact on encapsulation stability. From the application standpoint, these findings could have implications in many areas. For example, in drug delivery applications, the drug-loaded nanocarrier experiences both concentration and environmental changes upon biodistribution to diseased tissues. The mechanistic variations in two different environments provide insights into molecular designs that can afford stable encapsulation in one environment and release of the molecules in another.[32,33] Similarly, the results from this study may also provide new opportunities for designing nanoreactors[34,35] in which catalysts encapsulated in a host can be used to reversibly turn a chemical reaction on or off, because of the environment-dependent diffusion of reactant molecules.

ASSOCIATED CONTENT

Supporting Information

GPC and NMR spectra of the polymers, absorption spectra showing the calculation for cross-linking density of nanogels, fluorescence spectra for all dye exchange experiments, and tables for all leakage coefficients (Λ). This material is available free of charge via the Internet at http://pubs.acs.org.

AUTHOR INFORMATION

Corresponding Author

*E-mail: thai@chem.umass.edu.

Notes

The authors declare no competing financial interests.

ACKNOWLEDGMENTS

We thank the National Science Foundation (CHE- 1307118) and NIH (GM-065255) for support. We also thank the Center for Hierarchical Manufacturing for partial support (CMMI-1025020). We thank Brendan Abbott for repeating some of the experiments.

REFERENCES

(1) Allen, T. M.; Cullis, P. R. Drug Delivery Systems: Entering the Mainstream. *Science* **2004**, *303*, 1818–1822.
(2) Peer, D.; Karp, J. M.; Hong, S.; Farokhzad, O. C.; Margalit, R.; Langer, R. Nanocarriers as an Emerging Platform for Cancer Therapy. *Nat. Nanotechnol.* **2007**, *2*, 751–760.
(3) Oh, J. K.; Drumright, R.; Siegwart, D. J.; Matyjaszewski, K. The Development of Microgels/Nanogels for Drug Delivery Applications. *Prog. Polym. Sci.* **2008**, *33*, 448–477.
(4) Savic, R.; Eisenberg, A.; Maysinger, D. Block Copolymer Micelles as Delivery Vehicles of Hydrophobic Drugs: Micelle–Cell Interactions. *J. Drug Target.* **2006**, *14*, 343–355.
(5) Liu, K. C.; Yeo, Y. Extracellular Stability of Nanoparticulate Drug Carriers. *Arch. Pharmacal Res.* **2014**, *37*, 16–23.
(6) Kumar, R.; Chen, M. H.; Parmar, V. S.; Samuelson, L. A.; Kumar, J.; Nicolosi, R.; Yoganathan, S.; Watterson, A. C. Supramolecular Assemblies Based on Copolymers of PEG600 and Functionalized Aromatic Diesters for Drug Delivery Applications. *J. Am. Chem. Soc.* **2004**, *126*, 10640–10644.
(7) Pan, L.; He, Q.; Liu, J.; Chen, Y.; Ma, M.; Zhang, L.; Shi, J. Nuclear-Targeted Drug Delivery of TAT Peptide-Conjugated Monodisperse Mesoporous Silica Nanoparticles. *J. Am. Chem. Soc.* **2012**, *134*, 5722–5725.
(8) Shen, Y.; Jin, E.; Zhang, B.; Murphy, C. J.; Sui, M.; Zhao, J.; Wang, J.; Tang, J.; Fan, M.; Kirk, E. V.; Murdoch, W. J. Prodrugs Forming High Drug Loading Multifunctional Nanocapsules for Intracellular Cancer Drug Delivery. *J. Am. Chem. Soc.* **2010**, *132*, 4259–4265.
(9) Zhu, J.; Tan, M.; Zhang, L.; Yin, Q. Elongation Flow-Triggered Morphology Transitions of Dendritic Polyethylene Amphiphilic Assemblies: Host–Guest Implications. *Soft Matter* **2014**, *10*, 6506–6513.
(10) Rharbi, Y.; Winnik, M. A. Solute Exchange between Surfactant Micelles by Micelle Fragmentation and Fusion. *Adv. Colloid Interface Sci.* **2001**, *89*, 25–46.
(11) Piñeiro, L.; Freire, S.; Bordello, J.; Novo, M.; Al-Soufi, W. Dye Exchange in Micellar Solutions. Quantitative Analysis of Bulk and Single Molecule Fluorescence Titrations. *Soft Matter* **2013**, *9*, 10779–10790.
(12) Rharbi, Y.; Li, M.; Winnik, M. A.; Hahn, K. G. Temperature Dependence of Fusion and Fragmentation Kinetics of Triton X-100 Micelles. *J. Am. Chem. Soc.* **2000**, *122*, 6242–6251.
(13) Rharbi, Y.; Chen, L.; Winnik, M. A. Exchange Mechanisms for Sodium Dodecyl Sulfate Micelles: High Salt Concentration. *J. Am. Chem. Soc.* **2004**, *126*, 6025–6034.
(14) Novo, M.; Felekyan, S.; Seidel, C. A.; Al-Soufi, W. Dye-Exchange Dynamics in Micellar Solutions Studied by Fluorescence Correlation Spectroscopy. *J. Phys. Chem. B* **2007**, *111*, 3614–3624.
(15) Bordello, J.; Novo, M.; Al-Soufi, W. Exchange-Dynamics of a Neutral Hydrophobic Dye in Micellar Solutions Studied by

Fluorescence Correlation Spectroscopy. *J. Colloid Interface Sci.* **2010**, *345*, 369−376.
(16) Gehlen, M. H.; De Schryver, F. C. Time-Resolved Fluorescence Quenching in Micellar Assemblies. *Chem. Rev.* **1993**, *93*, 199−221.
(17) Jiwpanich, S.; Ryu, J.-H.; Bickerton, S.; Thayumanavan, S. Noncovalent Encapsulation Stabilities in Supramolecular Nanoassemblies. *J. Am. Chem. Soc.* **2010**, *132*, 10683−10685.
(18) Lu, J.; Owen, S. C.; Shoichet, M. S. Stability of Self-Assembled Polymeric Micelles in Serum. *Macromolecules* **2011**, *44*, 6002−6008.
(19) Dong, H.; Shu, J. Y.; Dube, N.; Ma, Y.; Tirrell, M. V.; Downing, K. H.; Xu, T. 3-Helix Micelles Stabilized by Polymer Springs. *J. Am. Chem. Soc.* **2012**, *134*, 11807−11814.
(20) Kim, K.; Bae, B.; Kang, Y. J.; Nam, J.-M.; Kang, S.; Ryu, J.-H. Natural Polypeptide-Based Supramolecular Nanogels for Stable Noncovalent Encapsulation. *Biomacromolecules* **2013**, *14*, 3515−3522.
(21) Zou, P.; Chen, H.; Paholak, H. J.; Sun, D. Noninvasive Fluorescence Resonance Energy Transfer Imaging of in Vivo Premature Drug Release from Polymeric Nanoparticles. *Mol. Pharmaceutics* **2013**, *10*, 4185−4194.
(22) Dan, K.; Rajdev, P.; Deb, J.; Jana, S. S.; Ghosh, S. Remarkably Stable Amphiphilic Random Copolymer Assemblies: A Structure−Property Relationship Study. *J. Polym. Sci. A Polym. Chem.* **2013**, *51*, 4932−4943.
(23) Li, L.; Ryu, J.-H.; Thayumanavan, S. Effect of Hofmeister Ions on the Size and Encapsulation Stability of Polymer Nanogels. *Langmuir* **2013**, *29*, 50−55.
(24) Fuller, J. M.; Raghupathi, K. R.; Ramireddy, R. R.; Subrahmanyam, A. V.; Yesilyurt, V.; Thayumanavan, S. Temperature-Sensitive Transitions below LCST in Amphiphilic Dendritic Assemblies: Host−Guest Implications. *J. Am. Chem. Soc.* **2013**, *135*, 8947−8954.
(25) Swaminathan, S.; Fowley, C.; McCaughan, B.; Cusido, J.; Callan, J. F.; Raymo, F. M. Intracellular Guest-Exchange between Dynamic Supramolecular Hosts. *J. Am. Chem. Soc.* **2014**, *136*, 7907−7913.
(26) Ghosh, S.; Basu, S.; Thayumanavan, S. Simultaneous and Reversible Functionalization of Copolymers for Biological Applications. *Macromolecules* **2006**, *39*, 5595−5597.
(27) Li, L.; Raghupathi, K.; Yuan, C.; Thayumanavan, S. Surface Charge Generation in Nanogels for Activated Cellular Uptake at Tumor-Relevant pH. *Chem. Sci.* **2013**, *4*, 3654−3360.
(28) Gjaltema, A.; Van Loosdrecht, M. C. M.; Heijnen, J. Abrasion of Suspended Biofilm Pellets in Airlift Reactors: Effect of Particle Size. *J. Biotechnol. Bioeng.* **1997**, *55*, 206−215.
(29) Yu, S.; Hu, J.; Pan, X.; Yao, P.; Jiang, M. Stable and pH-Sensitive Nanogels Prepared by Self-Assembly of Chitosan and Ovalbumin. *Langmuir* **2006**, *22*, 2754−2759.
(30) Kalyanasundaram, K.; Thomas, J. Environmental Effects on Vibronic Band Intensities in Pyrene Monomer Fluorescence and Their Application in Studies of Micellar Systems. *J. Am. Chem. Soc.* **1977**, *99*, 2039−2044.
(31) Bickerton, S.; Jiwpanich, S.; Thayumanavan, S. Interconnected Roles of Scaffold Hydrophobicity, Drug Loading, and Encapsulation Stability in Polymeric Nanocarriers. *Mol. Pharmaceutics* **2012**, *9*, 3569−3578.
(32) Du, J. Z.; Sun, T. M.; Song, W. J.; Wu, J.; Wang, J. A Tumor-Acidity-Activated Charge-Conversional Nanogel as an Intelligent Vehicle for Promoted Tumoral-Cell Uptake and Drug Delivery. *Angew. Chem., Int. Ed.* **2010**, *49*, 3621−3626.
(33) Poon, Z.; Chang, D.; Zhao, X. Y.; Hammond, P. T. Layer-by-Layer Nanoparticles with a pH-Sheddable Layer for in Vivo Targeting of Tumor Hypoxia. *ACS Nano* **2011**, *5*, 4284−4292.
(34) Wang, X.; Liu, G.; Hu, J.; Zhang, G.; Liu, S. Concurrent Block Copolymer Polymersome Stabilization and Bilayer Permeabilization by Stimuli-Regulated "Traceless" Crosslinking. *Angew. Chem., Int. Ed.* **2014**, *53*, 3138−3142.
(35) Yuan, C.; Luo, W.; Zhong, L.; Deng, H.; Liu, J.; Xu, Y.; Dai, L. Au @ Polymer Nanostructures with Tunable Permeability Shells for Selective Catalysis. *Angew. Chem., Int. Ed.* **2011**, *51*, 3515−3519.